Physical Properties of Charge Transfer Salt (EDO-TTFBr$_2$)$_2$AsF$_6$ in Mott Insulating State

Naoki Yoneyama, Akira Miyazaki, Toshiaki Enoki,* Eiji Ogura,† Yoshiyuki Kuwatani,† and Masahiko Iyoda†

Department of Chemistry, Graduate School of Science and Technology, Tokyo Institute of Technology, Ookayama, Meguro-ku, Tokyo 152-8551

†Department of Chemistry, Graduate School of Science, Tokyo Metropolitan University, Hachiohji, Tokyo 192-0397

(Received June 16, 1999)

We have investigated the physical properties of a new charge transfer salt based on an asymmetric donor 4,5-dibromo-4′,5′-ethylenedioxy-tetrathiafulvalene (EDO-TTFBr$_2$) whose crystal structure contains a weakly dimerized donor stacking structure. This salt is considered to be in a Mott insulating state in the vicinity of the metal-insulator boundary, taking account of the highly conductive semiconducting behavior and the feature of the susceptibility explained by the one-dimensional Heisenberg antiferromagnet model with an $S = 1/2$ localized spin per dimer and a large exchange interaction of about -190 K. The large exchange interaction and the exceptionally small resistivity (0.06 Ω cm at room temperature) originate from the strong inter-dimer transfer integral. The results of the ESR not only suggest an antiferromagnetic transition at 37 K, but also reflect the one-dimensional electronic state giving a negligible contribution to the spin-lattice relaxation process.

Among a large number of 4,5;4′,5′-bis(ethylenedithio)-tetrathiafulvalene (BEDT-TTF)-based charge transfer salts having low-dimensional electronic structures, there is a group of materials classified as Mott insulators,[1—3] where π-electrons are localized to give localized spins under the influence of the strong on-site Coulomb interaction. Accordingly, the charge transfer salts in the Mott insulating state are expected to form low-dimensional magnet systems with localized spins. At the same time, the important point which has to be added in characterizing the BEDT-TTF-based Mott insulators is a commonly observed structural feature that their crystal structures are formed with dimerized BEDT-TTF units. From this point of view, we have investigated the magnetic properties of several BEDT-TTF charge transfer salts in relation to the strength of the dimerization of donor molecules.[4] The previous study suggests that the strength of the donor dimerization crucially determines the degree of the localization/delocalization of the carriers in the Mott insulating regime, where, actually, there is a contrast between two charge transfer salts, β'-(BEDT-TTF)$_2$ICl$_2$ with a strong dimerization and α'-(BEDT-TTF)$_2$IBr$_2$ with a weak dimerization. However, it still remains unsolved what happens in the cases with the intermediate strengths of dimerization.

Recently a new asymmetric donor molecule of 4,5-dibromo-4′,5′-ethylenedioxytetrathiafulvalene (EDO-TTFBr$_2$) shown in Fig. 1(a) has been synthesized.[5] Asymmetric donor salts generally tend to form dimerized donor molecule units, and thus we picked out this salt as one of our target materials, since the results of preliminary experiments suggested that this salt would be a Mott insulating state having intermediate strength of the dimerization. In this paper we report the crystal structure, the resistivity, the susceptibility, and the ESR measurements.

Experimental Single crystals were synthesized by means of electrocrystallization using EDO-TTFBr$_2$ (4 mg) and supporting electrolyte (n-C$_4$H$_9$)$_4$NAsF$_6$ (30 mg) in the solvent of 1,1,2-trichloroethane (15 ml) with a constant current of about 1 μA for 4 d. Typical samples had sharp needle shapes with the size of ca. $3\times0.4\times0.1$ mm^3 (corresponding to the c-, b^*-, and a^*-axes, respectively). The crystal structure was analyzed using a Rigaku AFC-7R four circle X-ray diffractometer with Mo $K\alpha$ radiation. The structure was solved with the direct methods which resulted in a final R factor of 0.035 for 2554 reflections.

The transfer integrals between donor molecules and the energy band structure at room temperature were calculated based on the tight-binding approximation using the extended Hückel Hamiltonian.[6—8] We carried out the resistivity measurement by a four-probe method at ambient pressure and at 9 kbar using a clamp-type high pressure cell. The magnetic susceptibility was measured under a magnetic field of 10 kOe using a SQUID magnetometer (Quantum Design, MPMS-5) in the temperature range 1.7—300 K. About 30 single crystals (ca. 0.5 mg) were aligned in the same directions using Apiezon N grease. The spin susceptibility was obtained after the subtraction of the Pascal diamagnetic contribution of -4.99×10^{-4} emu mol^{-1} and a fractional Curie-tail at low temperatures coming from magnetic impurities (0.4 %). The ESR measurement was carried out with a single crystal, using an X-band ESR spectrometer (JEOL JES-TE200) in the

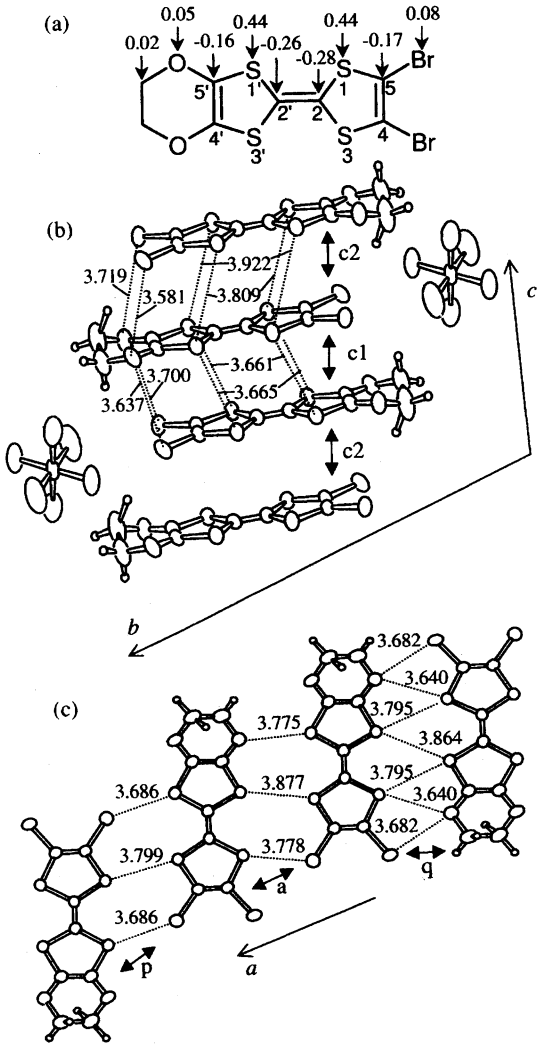

Fig. 1. (a) Molecular structure of EDO-TTFBr$_2$. Calculated HOMO coefficients are indicated by numerals with arrows. (b) and (c) The crystal structure of (EDO-TTFBr$_2$)$_2$AsF$_6$; the view of the donor stacking structure projected on the *bc*-plane (b) and the view along the side-by-side direction (c). Dotted lines are the inter-molecular atomic distances and double arrows indicate the molecular pairs connected by transfer integrals a, c1, c2, p, and q (see Fig. 2). The numbers indicate the inter-molecular atomic distances (Å).

temperature range 4.2—300 K.

Results

The crystallographic data and the atomic coordinates with thermal parameters are summarized in Tables 1 and 2, respectively. The crystal structure is shown in Figs. 1(b) and 1(c). A head-to-tail arrangement of asymmetric donor molecules is formed in the direction of face-to-face molecular contacts along the *c*-axis, where the shortest intermolecular S–S atomic contact 3.661 Å is almost the same as the corresponding van der Waals distance[9] 3.60 Å. There is no sufficient contact between Br and S/O atoms, whose shortest Br–O distance is 3.581 Å ($\gg$ the van der Waals distance 3.37 Å). In the side-by-side direction along the *a*-axis as shown in

Table 1. Crystallographic Data of (EDO-TTFBr$_2$)$_2$AsF$_6$

Formula	$(C_8H_4S_4O_2Br_2)_2AsF_6$
Crystal system	Triclinic
Space group	$P\bar{1}$
a/Å	7.099(5)
b/Å	14.844(4)
c/Å	7.019(3)
α/°	93.16(4)
β/°	106.07(6)
γ/°	79.81(8)
V/Å^3	699.9(8)
Z	2
Observed reflections ($I > 2\sigma(I)$)	2554
R	0.035

Table 2. Atomic Parameters of (EDO-TTFBr$_2$)$_2$AsF$_6$

Atom	x	y	z	B_{eq} (Å^2)
S1	0.62046(15)	0.31489(7)	0.7416(2)	2.77(2)
S2	0.19761(14)	0.40244(7)	0.6432(2)	2.76(2)
S3	0.74203(14)	0.52008(7)	0.8199(2)	2.64(2)
S4	0.31504(14)	0.59787(7)	0.7101(2)	2.86(2)
C1	0.4474(6)	0.4150(3)	0.7135(6)	2.41(6)
C2	0.4974(5)	0.5001(3)	0.7444(6)	2.32(6)
C3	0.4411(6)	0.2440(3)	0.6776(6)	2.86(7)
C4	0.2496(6)	0.2839(3)	0.6340(6)	2.70(6)
C5	0.6759(6)	0.6389(3)	0.8266(6)	2.47(6)
C6	0.4828(6)	0.6737(3)	0.7775(6)	2.50(6)
C7	0.3447(11)	0.1047(4)	0.6859(15)	6.79(2)
C8	0.1529(10)	0.1434(4)	0.5607(12)	5.36(2)
O1	0.5045(5)	0.1540(2)	0.6787(6)	4.01(6)
O2	0.0927(5)	0.2399(2)	0.5857(5)	3.55(6)
Br1	0.88162(7)	0.70664(3)	0.90497(7)	3.31(10)
Br2	0.37195(7)	0.79700(3)	0.77951(7)	3.59(11)
As	0.0000	0.0000	0.0000	3.30(2)
F1	0.0539(6)	−0.1129(2)	0.0610(6)	5.82(8)
F2	−0.0938(8)	0.0265(3)	0.1981(7)	8.21(2)
F3	0.2270(6)	0.0180(3)	0.1349(8)	8.52(2)

The equivalent temperature factor $B_{eq} = \frac{4}{3}\sum U_{ij} a_i^* a_j^* \boldsymbol{a}_i \cdot \boldsymbol{a}_j$.

Fig. 1(c), there are intermolecular S–S and S–O contacts of 3.775 and 3.640 Å, respectively, which are a little longer than the van der Waals distances (3.60 and 3.32Å for S–S and S–O contacts, respectively). Thus, the crystal structure is characterized with a quasi two-dimensional donor layer structure consisting of the two-dimensional arrangement of one-dimensional donor chains along the *c*-axis, where the presence of anion sheets in the galleries makes the two-dimensional layers separated from each other. This structure is considered to be similar to that of (DIMET)$_2$AsF$_6$,[10] where DIMET is dimethylethylenedithiotetrathiafulvalene. It is worth noting that an antiferromagnetic transition is observed in (DIMET)$_2$X (X = SbF$_6$, AsF$_6$).[11] The transfer integral network in the donor sheet in the *ac*-plane is shown in Fig. 2(a). The transfer integrals t_{c1} and t_{c2} along the face-to-face direction are more than 5 times larger than those in the side-by-side directions, suggesting a one-dimensional feature in the electronic structure. In the one-dimensional chain, there is an alternation in the strengths of the trans-

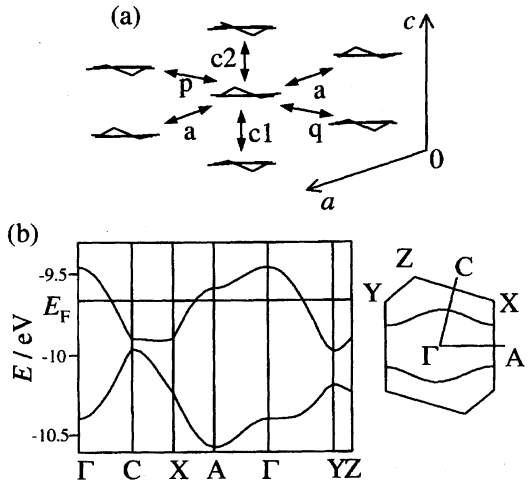

Fig. 2. (a) Schematic view of the crystal structure of (EDO-TTFBr$_2$)$_2$AsF$_6$ in the *ac*-plane. The inter-molecular transfer integrals are as follows; t_{c1} = 27.5, t_{c2} = 20.8, t_a = 3.85, t_p = 1.24, and t_q = -2.44×10^{-2} eV. (b) Band structure and Fermi surface.

fer integrals which is described in terms of dimerization in other words. The band structure is shown in Fig. 2(b), where the Fermi level is located around the mid-point of the upper band according to the 2 : 1 donor-to-anion ratio, and the presence of a one-dimensional Fermi surface along the c^*-axis is consistent with the crystal structure.

The temperature dependence of the resistivity shown in Fig. 3 is semiconductive with a room temperature resistivity of about 0.06 Ω cm and an activation energy of 0.13±0.01 eV. The pressure dependence of the resistivity at room temperature is shown in the inset of Fig. 3. The resistivity decreases monotonously as the pressure increases. The temperature dependence of the resistivity under pressure is also semiconductive even at 9 kbar with an activation energy of 0.09±0.01 eV, as shown in Fig. 3.

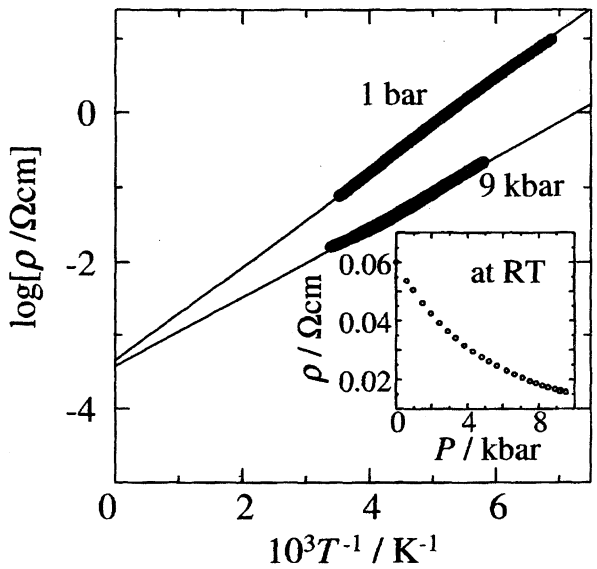

Fig. 3. Temperature dependence of the resistivity for (EDO-TTFBr$_2$)$_2$AsF$_6$. The solid lines are the Arrhenius fittings with activation energies of 0.13 and 0.09 eV at ambient pressure and 9 kbar, respectively. The inset shows the resistivity change under pressure.

Figure 4 shows the temperature dependence of the susceptibility with a field parallel to the *c*-axis. The susceptibility, whose room temperature value is about $5.5\pm0.5\times10^{-4}$ emu mol^{-1}, is gradually reduced as the temperature is lowered down to about 35 K, at which an anomaly appears. It should be noted that the anomaly is observed in the susceptibility which has been obtained by subtracting a Curie-type impurity contribution from the experimental result (see the inset of Fig. 4).

The ESR signal is Lorentzian with the peak-to-peak line width of about 20 Oe at room temperature. The ESR signal intensity shown in Fig. 5(a) obeys the temperature dependence of the susceptibility in the high temperature range down to 45 K. It gets small below about 40 K and vanishes below 37 K with the *g*-value shift, as shown in Fig. 5(b). The temperature dependence of the line width is shown in Fig. 5(c). It becomes narrow as the temperature is lowered down to 45 K, followed by an upturn below 45 K which diverges at 37 K.

Discussion

The temperature dependence of the resistivity indicates a typical activation process as an insulator, in contradiction to the metallic band structure predicted in Fig. 2, while the room temperature value of about 0.06 Ω cm is remarkably small

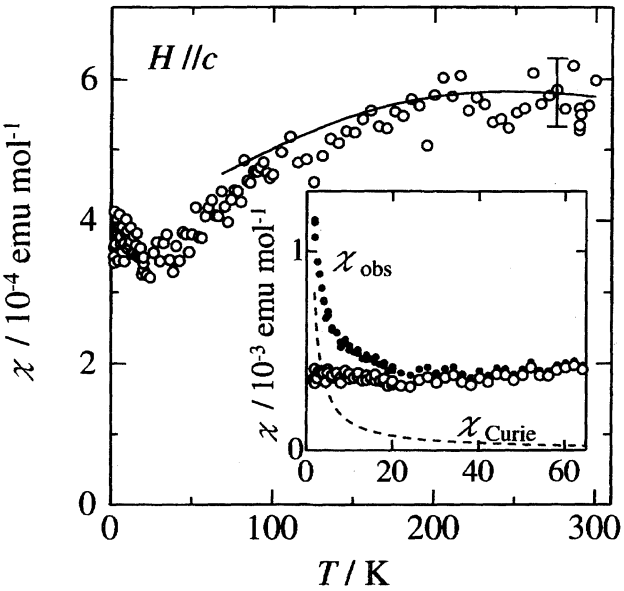

Fig. 4. Temperature dependence of the susceptibility measured at H = 10 kOe for (EDO-TTFBr$_2$)$_2$AsF$_6$ with an error bar of about $\pm0.5\times10^{-4}$ emu mol^{-1}. The solid curve is the fitting result for the S = 1/2 one-dimensional Heisenberg antiferromagnet model with J = −190 K. The inset shows the details at low temperatures. The susceptibility (open circle) is obtained from the observed susceptibility χ_{obs} (closed circle) after the subtraction of an impurity Curie tail, χ_{Curie} (broken curve), where the Curie constant is estimated at 1.3×10^{-4} emu^{-1} mol K^{-1}.

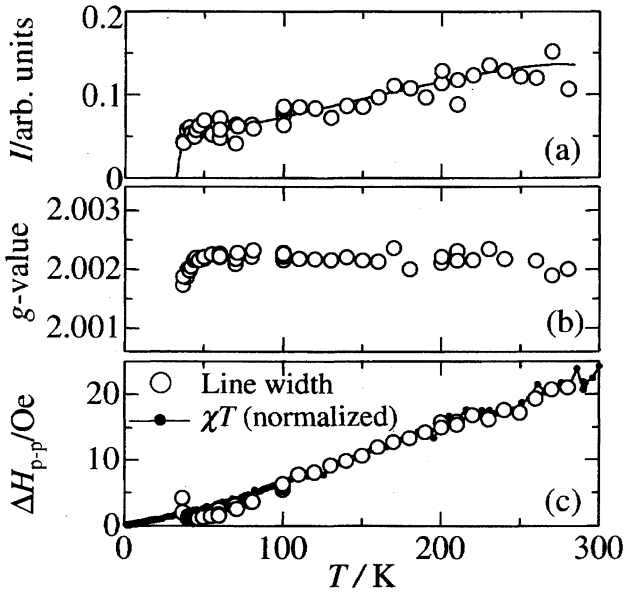

Fig. 5. Temperature dependence of the ESR data with the field parallel to the *c*-axis for $(EDO\text{-}TTFBr_2)_2AsF_6$. (a) ESR intensity *I*. The solid curve is a guide for the eyes. (b) The *g*-value. (c) The peak-to-peak ESR line width. The closed dot with the solid curve is the normalized χT product where χ is the spin susceptibility shown in Fig. 4. The value of χT at 280 K is normalized to the value of the line width at the same temperature.

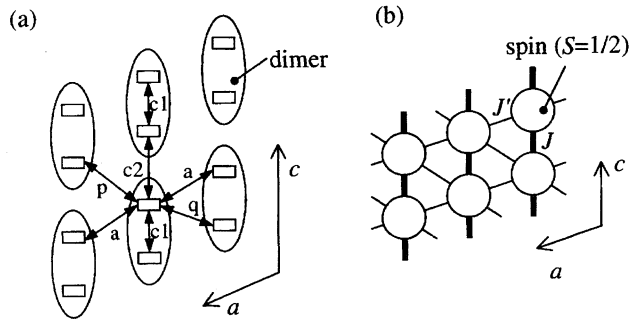

Fig. 6. Schematic structure of $(EDO\text{-}TTFBr_2)_2AsF_6$. (a) A rectangle represents a EDO-$TTFBr_2$ molecule viewed along the molecular long axis and an ellipsoid circling two molecules represents a dimer unit. (b) Magnetic structure predicted from Fig. 6(a). A circle represents a magnetic unit consisting of a dimer with an $S = 1/2$ spin and a line linking the circles represents an exchange interaction, where the strengths of the interactions are on the order of bold solid line (J) > thin solid line (J').

compared with insulators already investigated, suggesting that the electronic structure is situated in the vicinity of the metal-insulator boundary. High pressure investigation still shows semiconductive behavior even at 9 kbar, although the activation energy is reduced by about 30% from the value at ambient pressure. In addition to the semiconductive behavior, the presence of localized magnetic moments, which we will see later, proves that the electronic state of this salt is described as a magnetic semiconductor in the Mott insulating state. On the basis of the resistivity vs susceptibility diagram which gives a criterion for a Mott insulator as presented in Ref. 4, this salt is placed empirically in the boundary region between the Mott insulating regime and the metallic regime, although the calculated band structure shown in Fig. 2(b) slightly deviates from a simple effective half-filled band structure, which is a requisite for a Mott insulator.

We here reexamine the structural features to consider the small resistivity and the magnetic properties of this salt. Figure 6(a) shows the schematic structure of the donor molecule arrangement. The transfer integrals t_{c1} and t_{c2} form a one-dimensional stacking structure along the *c*-axis. The intra-dimer transfer integral t_{c1} is larger than the inter-dimer transfer integrals, where the ratio of the intra-dimer to the largest inter-dimer transfer integral t_{c2} is estimated at $t_{intra}/t_{inter} = t_{c1}/t_{c2} = 1.3$. Therefore, the dimerization is considered to have a moderately weak strength compared with the strong dimerization of β'-$(BEDT\text{-}TTF)_2ICl_2$ ($t_{intra}/t_{inter} = 2.7$) and the weak dimerization of α'-$(BEDT\text{-}TTF)_2IBr_2$ ($t_{intra}/t_{inter} = 1.2$).[4] The other transfer integrals, t_a, t_p, and t_q, which are characterized with the side-by-side inter-molecular atomic contacts, are an order of magnitude weaker than the intra-chain transfer integrals. Thus, from the viewpoint of the localized model, the magnetic structure based on the dimer unit is expected to be a quasi one-dimensional structure, as shown in Fig. 6(b). The small resistivity (ca. 0.06 Ω cm at room temperature) can be attributed to the large inter-dimer transfer integral t_{c2} (= 208 meV).

The susceptibility has a value of about 5.5×10^{-4} emu mol^{-1} at room temperature, which is in between the value for a localized spin system in insulating state and that for a conduction electron system in metallic state. The highly conductive semiconducting behavior and the small paramagnetic susceptibility obviously indicate a Mott insulating state located in the vicinity of the metal-insulator boundary. The temperature dependence of the susceptibility shows a gradual decrease as the temperature is lowered. This behavior cannot be fitted to the Curie–Weiss law, which makes difficult a quantitative estimation of the localized spin density. We here try to fit the temperature dependence of the susceptibility above ca. 100 K to the one-dimensional Heisenberg antiferromagnet model[12] as depicted with the solid curve of Fig. 4, where we neglect the contribution of the inter-chain interaction. The result of the fitting gives an intra-chain exchange interaction of $J = -190\pm25$ K with a magnetic moment of 1.73 μ_B per formula unit, which corresponds to an $S = 1/2$ spin when we employ $g = 2.002$ from the ESR result. The fitting indicates a good quantitative agreement with the experimental data, so the experimental finding suggests the existence of almost an $S = 1/2$ spin per dimer, where the antiferromagnetic exchange interaction ranging about 200 K works between localized spins. Taking into account that the exchange interaction is expressed by $J \approx -t^2/U$, the strong exchange interaction is explained by the large value of the dominant inter-dimer transfer integral t_{c2} which connects two dimer units one-dimensionally along the *c*-axis.

The temperature dependence of the ESR intensity is qualitatively consistent with the static susceptibility at high tem-

peratures, while the ESR signal disappears below 37 K accompanied by a divergent upturn of the line width. Additionally, the g-value is shifted down steeply just above 37 K. Consequently, the ESR experimental results suggest the onset of an antiferromagnetic ordering at T_N = 37 K. The observed susceptibility in the field parallel to the c-axis that has a finite value even well below T_N can be explained by the behavior of the perpendicular susceptibility in the antiferromagnetic ordered state. If this is the case, the estimation of the intra-chain exchange interaction J is also possible using the value of the perpendicular susceptibility at 0 K, $\chi_\perp(0)$. According to the spin wave theory,[13] $\chi_\perp(0)$ is expressed as

$$\chi_\perp(0) \approx \chi_\perp^0[1 - \Delta S/S - e(0)/2zS], \quad (1)$$

for a system with $H_A \ll H_E$ where H_A is the magnetic anisotropy field and H_E is the exchange field. $\chi_\perp^0$ is the temperature-independent perpendicular susceptibility based on the molecular field theory, $\chi_\perp^0 = Ng^2\mu_B^2/4zJ$, z is the number of the nearest neighbors, $\Delta S/S$ is the spin reduction term for the sublattice magnetization, and $e(0)/2zS$ is the correction for the real ground state spin energy. In the present case with the value extrapolated to 0 K, which is estimated at $\chi_\perp(0) \approx 4 \pm 1 \times 10^{-4}$ emu mol^{-1}, the relation described in Eq. 1 gives a value of the inter-chain interaction $J \approx -150 \pm 50$ K, using the values[13] of $\Delta S/S = 0.350$, $e(0) = 0.69$, $z = 2$. The obtained value of J is in good quantitative agreement with $J \approx -190$ K estimated from the higher temperature region.

The ESR line width is a good indicator for characterizing the electron transport process. According to the previous paper which reported the correlation between the linewidth and the electron localization/delocalization of the dimer-based charge transfer salts in the Mott insulating state,[4] the behavior of the line width shows different features depending on the degree of electron delocalization that is well correlated to the strength of dimerization, although static susceptibility can be described in terms of the localized spin scheme irrespective of the degree of electron delocalization. The contribution of the spin–lattice relaxation becomes dominant to the line width of the delocalized electronic system, which is related to the relaxation time of carriers in the conduction process. α'-(BEDT-TTF)$_2$IBr$_2$ having a small resistivity (ca. 0.5 Ω cm)[1] is a typical example with a delocalized electronic system, which has a wide line width of about 60 Oe at room temperature.[14] Meanwhile, in the localized electronic systems, the spin–spin relaxations governed by the dipole–dipole interaction play a major role in the line width where the line width is subjected to the exchange-narrowing mechanism in an exchange-interaction-networked localized spin system. β'-(BEDT-TTF)$_2$ICl$_2$ shows a typical behavior in this regime, having a room temperature resistivity value of about 20 Ω cm and the narrow ESR line width of ca. 10 Oe. Moreover, from the spin-diffusion theory[15] of the spin–spin relaxation mechanism, the combination of the dipole–dipole and exchange interactions makes the line width be proportional to χT at high temperatures in low-dimensional magnets. Actually, the β'-salt indicates a good correlation with the behavior of χT product.[4] The same comparison between the ESR line width and the χT product for (EDO-TTFBr$_2$)$_2$AsF$_6$ is shown in Fig. 5(c). Taking account of the remarkably high conductivity even in the semiconducting state and the narrow line width, the excellent correlation between the line width and χT in Fig. 5(c) seems to be exceptional. However, if we pinpoint the dimensionality in the electronic structure of (EDO-TTFBr$_2$)$_2$AsF$_6$, the exceptional feature in the correlation can be explained reasonably. The transfer integrals obtained for (EDO-TTFBr$_2$)$_2$AsF$_6$ give an almost purely one-dimensional electronic feature in contrast to the BEDT-TTF Mott systems already investigated. According to the spin-lattice relaxation theory,[16] no spin–lattice relaxation process is allowed in ideal one-dimensional conductors. Eventually, the excellent correlation revealed in the present case suggests the ineffectiveness of the spin–lattice relaxation process in the donor one-dimensional electronic system.

In conclusion, we have investigated the physical properties of an asymmetric donor salt (EDO-TTFBr$_2$)$_2$AsF$_6$. The crystal structure features a one-dimensional dimerized donor stacking along the c-axis. This salt is considered to be in a Mott insulating state in the vicinity of the metal-insulator boundary, taking account of the highly conductive semiconducting behavior and the feature of the susceptibility explained with the one-dimensional Heisenberg antiferromagnet model with an $S = 1/2$ localized spin per dimer and a large exchange interaction of about −190 K. The moderately weak dimerization is considered to give almost one localized spin to a dimerized donor unit. The result of the ESR suggests the presence of an antiferromagnetic transition at 37 K. The correlation between the line width and the χT indicates the feature of the one-dimensional electronic state giving negligible contribution of the spin–lattice relaxation process. These experimental findings with the presence of localized spins and the exceptionally good conductive feature are ascribed to a moderately dimerized structure of this salt, in contrast with the behavior of the strongly dimerized β'-type salt and the weakly dimerized α'-type salts.

This work is supported by a Grant-in-Aid for Scientific Research on Priority Areas No. 10149101 "Metal-assembled Complexes" from the Ministry of Education, Science, Sports and Culture.

References

1 M. Tokumoto, H. Anzai, T. Ishiguro, G. Saito, H. Kobayashi, R. Kato, and A. Kobayashi, *Synth. Met.*, **19**, 215 (1987).

2 S. D. Obertelli, R. H. Friend, D. R. Talham, M. Kurmoo, and P. Day, *J. Phys.: Condens. Matt.*, **1**, 5671 (1989).

3 M. Kurmoo, M. Allan, R. H. Friend, D. Chasseau, G. Bravic, and P. Day, *Synth. Met.*, **41-43**, 2127 (1991).

4 N. Yoneyama, A. Miyazaki, T. Enoki, and G. Saito, *Bull. Chem. Soc. Jpn.*, **72**, 639 (1999).

5 M. Iyoda, E. Ogura, T. Takano, K. Hara, Y. Kuwatani, T. Kato, N. Yoneyama, J. Nishijyo, A. Miyazaki, and T. Enoki, *J.*

Chem. Soc., Chem. Commun., submitted.

6 T. Mori, A. Kobayashi, Y. Sasaki, H. Kobayashi, G. Saito, and H. Inokuchi, *Bull. Chem. Soc. Jpn.*, **57**, 627 (1984).

7 R. H. Summerville and R. Hoffmann, *J. Am. Chem. Soc.*, **98**, 7240 (1976).

8 For oxygen and bromine, the exponents of the Slater-type orbitals (ζ) and the ionization potentials (ϵ) are as follows; ζ = 2.275 (for O 2s, 2p) and 2.054 (Br 4s, 4p); $\epsilon = -32.4$ (O 2s), -15.9 (O 2p), -24.1 (Br 4s), and -12.5 (Br 4p) eV, respectively (C. J. Ballhausen and H. B. Gray, "Molecular Orbital Theory," W. A. Benjamin, (1964), p. 122).

9 A. Bondi, *J. Phys. Chem.*, **68**, 441 (1964).

10 B. Gallois, J. Gaultier, F. Bechtel, D. Chasseau, C. Hauw, and L. Ducasse, *Synth. Met.*, **19**, 419 (1987).

11 R. Laversanne, C. Coulon, J. Amiell, E. Dupart, P. Delhaes, J. P. Morand, and C. Manigand, *Solid State Commun.*, **58**, 765 (1986).

12 J. C. Bonner and M. E. Fisher, *Phys. Rev.*, **135**, A640 (1964).

13 F. Keffer, "Encyclopedia of Physics," ed by H. P. J. Wijn, Springer-Verlag, New York (1966), Vol. XVIII 2, p. 124.

14 N. Kinoshita, M. Tokumoto, H. Anzai, and G. Saito, *Synth. Met.*, **19**, 203 (1987).

15 Y. Ajiro, S. Matsukawa, T. Yamada, and T. Haseda, *J. Phys. Soc. Jpn.*, **39**, 259 (1975).

16 R. J. Elliott, *Phys. Rev.*, **96**, 266 (1954).